A Stabilized Sequential Coupling Algorithm for Hydro-mechanical Systems using Reproducing Kernel Particle Method

Yongning XIE[1], Gang WANG[1,*]

[1] Department of Civil and Environmental Engineering
The Hong Kong University of Science and Technology, Hong Kong SAR, China
* Corresponding author: gwang@ust.hk

Abstract Sequential coupling scheme is a flexible numerical scheme to solve a coupled hydro-mechanical system. However, it suffers from severe numerical instability. Stability analysis of a sequential coupling scheme is performed in this paper. It is derived that the numerical scheme can be unconditionally stable with a stabilization term introduced to the fluid equation, while it is only conditionally stable without the stabilization. Reproducing Kernel Particle Method (RKPM) is used for spatial discretization. One dimensional consolidation in an elastic medium is conducted to verify the sequential scheme, and the convergence behavior during the iterations is presented.

Keywords hydro-mechanical coupling, sequential, meshfree, stability

1. Introduction

Sequential coupling scheme has been extensively studied in the past decades to solve the coupled hydro-mechanical system (*e.g.* [1-4]). It has great advantage over the traditional fully-coupled numerical scheme due to its *modularity* such that the fluid and the mechanical solver for corresponding governing equations can be executed separately without many extra manipulations. The coupling effect is fulfilled through the information exchange between two solvers. *Modularity* is particularly advantageous in practical applications. However, the convenience does not come without any price. The numerical stability and convergence is one problem frequently encountered using the sequential scheme. As has been demonstrated in literatures, different sequential algorithms require different stability conditions [4].

One part of this work is to seek a stable sequential couplings scheme. It is worth pointing out that the current study only focuses on the stability and convergence problem in the temporal space. To achieve this goal, a stabilization term is introduced to the fluid equation. Using the conventional stability analysis, it is found that the scheme can be unconditionally stable with a suitably chosen relaxation parameter. Another part of the work is to employ one type of meshfree methods, Reproducing Kernel Particle Method (RKPM), for spatial discretization. Due to their high order interpolations and *mesh-free* nature, meshfree methods are generally considered to have advantage in handling problems with large strains or strain localization. These features are not demonstrated in this paper as the emphasis is more on the formulation and stability of the sequential scheme. However, the numerical results do suggest the applicability of RKPM to the coupling scheme developed. More interesting features of RKPM may show up if nonlinear constitutive models are used and more complicated boundary value problems considered.

This paper is arranged as follows: Governing equations for the hydro-mechanical system are presented first, followed by the spatial discretization by RKPM and algorithm of sequential scheme. Stability analysis of the numerical scheme is presented subsequently. Numerical simulations for verification of the stability conditions are then demonstrated.

Throughout the paper, letter in bold face denotes tensor or vector. $()_{,i}$ denotes partial derivative with respect to coordinate. A superscript dot over a variable $\dot{()}$ denotes the time derivative of that variable. δ_{ij} is the Kronecker delta tensor.

2. Governing Equations

The coupled formulation of fully saturated porous media used in this work is so-called $\mathbf{u}-p$ formulation, in which the displacement of solid $\mathbf{u}$ and pore fluid pressure p are treated as two primary unknown variables [5]. The governing equations are derived from the equation of momentum equilibrium of solid-fluid mixture and equation of mass conservation of fluid as follows:

$$(\sigma'_{ij} - p\delta_{ij})_{,j} - \rho\ddot{u}_i + \rho b_i = 0 \tag{1}$$

$$\left(k_{ij}(-p_{,j} + \rho_f b_j)\right)_{,i} + \dot{\varepsilon}_{ii} + \frac{n\dot{p}}{K_f} = 0 \tag{2}$$

where σ'_{ij} is the effective stress tensor, which is related to the total stress σ_{ij} and pore fluid pressure p via $\sigma'_{ij} = \sigma_{ij} + p\delta_{ij}$. The effective stress in tension and pressure in compression are assigned with positive sign. ρ and ρ_f are the mass densities of the mixture and fluid, respectively. b_i is unit body force, k_{ij} is permeability tensor, which has a dimension of $[\text{length}]^3[\text{time}]/[\text{mass}]$ and is related to the conventional permeability k'(dimension: $[\text{length}]/[\text{time}]$) by $k = k'/\rho_f g$; ε_{ij} is the strain tensor; n is the porosity; K_f is the bulk modulus of the fluid. It should be noted that the governing equations presented here are simplified from [5] with the assumption that solid grains are incompressible.

The effective stress σ'_{ij} can be calculated from the constitutive relationship in rate form as follows:

$$\dot{\sigma}'_{ij} = C_{ijkl}\dot{\varepsilon}_{kl} \tag{3}$$

where C_{ijkl} is the tangent modulus of the solid and ε_{ij} is strain tensor.

The solid-fluid behaviors are coupled in that changing pore pressure influences the mechanical equilibrium state of the mixture, and the volumetric strain rate of the mixture affects the mass balance of the fluid. While the coupling problem can be approximated and solved in a decoupled manner in some special cases, the coupling effect is an important for a strongly coupled hydro-mechanical system and it cannot be neglected.

3. Spatial Discretization with RKPM

Denote $\mathbf{N}^u$ and $\mathbf{N}^p$ as the shape functions for displacement $\mathbf{u}$ and pore water pressure p, respectively. The semi-discrete form of the governing equations (1) and (2) can be obtained by multiplying the governing equations (1) and (2) by $\left(\mathbf{N}^u\right)^T$ and $\left(\mathbf{N}^p\right)^T$ respectively, followed by integration by part:

$$\mathbf{M}\ddot{\mathbf{u}} + \mathbf{K}\mathbf{u} - \mathbf{Q}\mathbf{p} - \mathbf{f}^u = 0 \tag{4}$$

$$\mathbf{Q}^T\dot{\mathbf{u}} + \mathbf{H}\mathbf{p} + \mathbf{S}\dot{\mathbf{p}} - \mathbf{f}^p = 0 \tag{5}$$

where

$\mathbf{M} = \int_\Omega (\mathbf{N}^u)^T \rho \mathbf{N}^u d\Omega$ (mass matrix); $\mathbf{K} = \int_\Omega \mathbf{B}^T \mathbf{C}\mathbf{B} d\Omega$ (stiffness matrix)

$\mathbf{f}^u = \int_{\Gamma_t} (\mathbf{N}^u)^T \bar{\mathbf{t}} d\Gamma_t + \int_\Omega (\mathbf{N}^u)^T \rho \mathbf{b} d\Omega$ (external forces)

$\mathbf{Q} = \int_\Omega \mathbf{B}^T \mathbf{m} \mathbf{N}^p d\Omega$ (coupling matrix); $\mathbf{H} = \int_\Omega (\nabla \mathbf{N}^p)^T \mathbf{k} \nabla \mathbf{N}^p d\Omega$ (permeability matrix);

$\mathbf{S} = \int_\Omega (\mathbf{N}^p)^T \frac{n}{K_f} \mathbf{N}^p d\Omega$ (compressibility matrix); $\mathbf{f}^p = \int_\Omega (\nabla^T \mathbf{N}^p)(\mathbf{k}\rho_f \mathbf{b}) d\Omega + \int_{\Gamma_w} (\mathbf{N}^p)^T \bar{q} d\Gamma_w$

and $\mathbf{m} = [1\ 1\ 1\ 0\ 0\ 0]^T$, $\mathbf{B}$ is strain-displacement matrix (the spatial derivatives of the shape functions). The boundary conditions are $\mathbf{u} = \bar{\mathbf{u}}$ on displacement boundary $\mathbf{\Gamma}_u$ and $\mathbf{t} = \bar{\mathbf{t}}$ on traction boundary $\mathbf{\Gamma}_t$, $p = \bar{p}$ on pressure boundary $\mathbf{\Gamma}_p$ and $q = \bar{q} = -\boldsymbol{n}^T \boldsymbol{k}(-\nabla \boldsymbol{p} + \rho_f \boldsymbol{b})$ on flux boundary Γ_w. The total boundary $\mathbf{\Gamma} = \mathbf{\Gamma}_u \bigcup \mathbf{\Gamma}_t = \mathbf{\Gamma}_p \bigcup \mathbf{\Gamma}_w$. Proper initial boundary conditions should also be given for the numerical simulation to start off.

RKPM shape functions ([6,7]) are used in this study. The RKPM shape functions interpolate the solution over discrete nodes, which, unlike the conventional FEM, have no topological connectivity relationship. Here only the formulation of shape functions and essential boundary imposition are briefly introduced. Readers may refer to [6-8] for the detailed formulations and implementations.

Function $u(x)$ in the domain can be approximated by the following formulation

$$u(\boldsymbol{x}) = \int_\Omega u(\bar{\boldsymbol{x}}) K(\boldsymbol{x} - \bar{\boldsymbol{x}}; \tilde{\mathrm{n}}) d\bar{V} \tag{6}$$

where $u(\bar{\boldsymbol{x}})$ are the values of field variables at particles. $K(\boldsymbol{x} - \bar{\boldsymbol{x}}; \tilde{\mathrm{n}})$ is the compactly-supported kernel function formulated in RKPM as multiplication of a correction function $C(\boldsymbol{x}, \bar{\boldsymbol{x}})$ and a window function $\Phi(\boldsymbol{x} - \bar{\boldsymbol{x}})$, *i.e.*, $K(\boldsymbol{x} - \bar{\boldsymbol{x}}) = C(\boldsymbol{x}, \bar{\boldsymbol{x}})\Phi(\boldsymbol{x} - \bar{\boldsymbol{x}})$. The correction function $C(\boldsymbol{x}, \bar{\boldsymbol{x}})$ is assumed to be linear with respect to $(\boldsymbol{x} - \bar{\boldsymbol{x}})$. The window function may take the form of a cubic spline or Gaussian function and has a rectangular or circular support in 2D case. Accordingly, the displacement can be interpolated as

$$u^h(\boldsymbol{x}) = \sum_{J=1}^{NP} N_J(\boldsymbol{x}) u_J \tag{7}$$

where the reproducing kernel approximant (shape function) $N_J(\boldsymbol{x})$ is given by

$$N_J(\boldsymbol{x}) = C(\boldsymbol{x}, \boldsymbol{x}_J)\Phi(\boldsymbol{x} - \boldsymbol{x}_J)\Delta V_J \tag{8}$$

$\boldsymbol{x}_J$ and ΔV_J are the position and contributing volume of the Jth node, respectively. The RKPM shape function does not possess Kronecker delta property, *i.e.* $u^h(\boldsymbol{x}_I) \neq u_I$. Therefore, special treatment is required to impose the essential boundary conditions. In this paper, the essential boundary condition is reinforced by transformation method ([7]).

4. Sequential Coupling Scheme

There are numerous sequential coupling schemes with varied degrees of success in stability ([4]). This study introduces a simple stabilization term by considering the difference of pore fluid pressures between successive iterations. Rewrite the mechanics solver and fluid solver as follows:

$$\text{Mechanics Solver}: \quad \mathbf{M}\ddot{\boldsymbol{u}}_{n+1}^{(i+1,k+1)} + \mathbf{C}_{n+1}^{(i+1,k)} \dot{\mathbf{u}}_{n+1}^{(i+1,k)} + \mathbf{K}_{n+1}^{(i+1,k)} \mathbf{u}_{n+1}^{(i+1,k)} - \mathbf{Q}\mathbf{p}_{n+1}^{(i+1)} - \mathbf{f}_{n+1}^{u} = 0 \tag{9}$$

$$\text{Fluid Solver}: \left(\mathbf{H}\Delta t_f + \mathbf{S}\right)\mathbf{p}_{n+1}^{(i+1)} + \boxed{\tilde{\mathbf{S}}\left(\mathbf{p}_{n+1}^{(i+1)} - \mathbf{p}_{n+1}^{(i)}\right)} + \mathbf{Q}^T\left(\mathbf{u}_{n+1}^{(i)} - \mathbf{u}_n\right) - \mathbf{S}\mathbf{p}_n - \mathbf{f}_{n+1}^p \Delta t_f = 0 \qquad (10)$$

In the above equations, subscripts n and $n+1$ represent the real time t_n and t_{n+1}, respectively, $\Delta t_f = t_{n+1} - t_n$ is the time increment. $\mathbf{p}_n$ and $\mathbf{u}_n$ are solutions of pressure and displacement at t_n. The displacement rate in Eq.(5) is approximated as $\dot{\mathbf{u}}_{n+1} = \dfrac{\mathbf{u}_{n+1}^{(i)} - \mathbf{u}_n}{\Delta t_f}$. During the iterations within one step, the fluid solver and mechanics solver are executed sequentially, with iteration numbers denoted by superscripts i, $i+1$(e.g., $\mathbf{p}_{n+1}^{(i)}$, $\mathbf{p}_{n+1}^{(i+1)}$,$\mathbf{u}_{n+1}^{(i+1,*)}$). The flow solver solves the pressure at once implicitly, while the mechanics solver solves the displacement explicitly through iterations, denoted by superscripts k, $k+1$... (e.g. $\mathbf{u}_{n+1}^{(i+1,k)}$, $\mathbf{u}_{n+1}^{(i+1,k+1)}$).

The boxed term in the flow solver is added to stabilize the system. $\tilde{\mathbf{S}}$ is an introduced parameter which will be determined in order to satisfy the numerical stability requirement and to achieve an optimal convergence rate. The stabilization term is essentially a term related to the variation of pressure increment during successive iterations, which vanishes when $\mathbf{p}_{n+1}^{(i+1)} \to \mathbf{p}_{n+1}^{(i)}$ and a consistent solution of displacement and pore water pressure is consequently achieved. Without the stabilization term, the solution of Eq. (10) (*i.e.*$\mathbf{p}_{n+1}^{(i+1)}$) may be unstable or even unattainable, as will be demonstrated by stability analysis in Section 5.

The sequence of solver calling varies in different schemes ([4]). The sequential scheme in this study first updates the pore water pressure by calling the flow solver, and then updates the displacement using the mechanical solver. Nested numerical iterations (denoted using subscript n and superscripts i, k) are required to solve the system. The general procedure is listed as the following.

(1). Initialization at the start of time: $\mathbf{p}_0 = \mathbf{p}_{ini}$, $\mathbf{u}_0 = \mathbf{u}_{ini}$.

(2). Start time integration $n = 0$

(a) Initialization $\mathbf{p}_{n+1}^{(0)} = \mathbf{p}_n$, $\mathbf{u}_{n+1}^{(0)} = \mathbf{u}_n$, update $\mathbf{f}_{n+1}^u$ and $\mathbf{f}_{n+1}^p$.

(b) Start iteration scheme $i = 0$.

i. Call flow solver to solve for $\mathbf{p}_{n+1}^{(i+1)}$:

$$\mathbf{p}_{n+1}^{(i+1)} = \left(\mathbf{H}\Delta t_f + \mathbf{S} + \tilde{\mathbf{S}}\right)^{-1}\left[\tilde{\mathbf{S}}\mathbf{p}_{n+1}^{(i)} - \mathbf{Q}^T\left(\mathbf{u}_{n+1}^{(i)} - \mathbf{u}_n\right) + \mathbf{S}\mathbf{p}_n + \mathbf{f}_{n+1}^p \Delta t_f\right]$$

ii. Call mechanics solver using predictor-corrector integration method. k starts from 0. $\mathbf{u}_{n+1}^{(1,0)} = \mathbf{u}_n$.

A. Compute the predictors:

$$\tilde{\mathbf{u}}_{n+1}^{(i+1,k+1)} = \mathbf{u}_{n+1}^{(i+1,k)} + \Delta t \mathbf{v}_{n+1}^{(i+1,k)} + \frac{(\Delta t)^2}{2}(1-2\beta)\ddot{\mathbf{u}}_{n+1}^{(i+1,k)}$$

$$\tilde{\mathbf{v}}_{n+1}^{(i+1,k+1)} = \mathbf{v}_{n+1}^{(i+1,k)} + (1-\gamma)\Delta t \ddot{\mathbf{u}}_{n+1}^{(i+1,k)}$$

$\Delta t = 10^{-5}$ s (pseudo-time step)

B. Update $\square_{n+1}^{(i+1,k+1)} = \int_\Omega \mathbf{B}^T \mathbf{C}\left(\nabla^s \tilde{\mathbf{u}}_{n+1}^{(i+1,k+1)}\right)\mathbf{B} d\Omega$ for nonlinear materials.

C. Compute $\ddot{\mathbf{u}}_{n+1}^{(i+1,k+1)} = \mathbf{M}^{-1}\left(\mathbf{Q}\mathbf{p}_{n+1}^{(i+1)} + \mathbf{f}_{n+1}^u - \tilde{\mathbf{C}}\tilde{\mathbf{v}}_{n+1}^{(i+1,k+1)} - \square_{n+1}^{(i+1,k+1)}\tilde{\mathbf{u}}_{n+1}^{(i+1,k+1)}\right)$

D. Compute the correctors:

$$\mathbf{u}_{n+1}^{(i+1,k+1)} = \tilde{\mathbf{u}}_{n+1}^{(i+1,k+1)} + \beta(\Delta t)^2 \ddot{\mathbf{u}}_{n+1}^{(i+1,k+1)}$$

$$\mathbf{v}_{n+1}^{(i+1,k+1)} = \tilde{\mathbf{v}}_{n+1}^{(i+1,k+1)} + \gamma \Delta t \ddot{\mathbf{u}}_{n+1}^{(i+1,k+1)}$$

E. Check whether $\frac{\| \mathbf{F}_{unbal} \|}{\| \mathbf{F}_{tot} \|} \le TOL_{unbal}$.

If *NO*, $k \Leftarrow k+1$ and go to (2)(b) iiA.

F. End mechanics solver. Commit $\mathbf{u}_{n+1}^{(i+1)} = \mathbf{u}_{n+1}^{(i+1,k+1)}$.

iii. Check whether both the solutions $\mathbf{p}_{n+1}^{(i+1)}$ and $\mathbf{u}_{n+1}^{(i+1)}$ satisfy the convergence criteria, *i.e.* $\left\|\mathbf{p}_{n+1}^{(i+1)} - \mathbf{p}_{n+1}^{(i)}\right\| \Big/ \left\|\mathbf{p}_{n+1}^{(i+1)}\right\| \le TOL_p$ and $\left\|\mathbf{u}_{n+1}^{(i+1)} - \mathbf{u}_{n+1}^{(i)}\right\| \Big/ \left\|\mathbf{u}_{n+1}^{(i+1)}\right\| \le TOL_u$. If *NO*, $i \Leftarrow i+1$, and go to (2)(b)i.

iv. End iteration scheme.

(c) Update $\mathbf{p}$ and $\mathbf{u}$: $\mathbf{p}_{n+1} = \mathbf{p}_{n+1}^{(i+1)}$ and $\mathbf{u}_{n+1} = \mathbf{u}_{n+1}^{(i+1)}$.

(d) If $n <$ total time step, $n \Leftarrow n+1$, and go to (2)(a).

(3). End time integration.

where $\mathbf{v} = \dot{\mathbf{u}}$ is the velocity vector, $\mathbf{F}_{unbal}$ is the unbalanced force, $\mathbf{F}_{tot}$ is the total applied force. $TOL_{unbal}, TOL_p, TOL_u$ are tolerance for the unbalance force, pore water pressure variation and displacement variation, respectively. β and γ are the two numerical parameters for the integration method. In the simulations presented in this paper, $\beta = 0.25, \gamma = 0.5$ are used. $\mathbf{C}$ is taken as the conventional Rayleigh damping given by $\mathbf{C} = a\mathbf{M} + b\mathbf{K}$.

As mentioned before, the mechanics and fluid solvers may employ different solution schemes. In the scheme proposed, the fluid solver is formulated using implicit integration for pressure, while mechanics solver solves displacement explicitly. The reason for this is that fluid solver is generally 'more' linear and can be efficiently solved while highly nonlinear constitutive model may be used in the mechanics solver which makes the implicit method much more difficult. Besides, in the mechanics solver, the mass matrix in step (2)(b)iiC can be approximated as a diagonally-lumped mass matrix, inversion of which can be readily obtained. The computation cost would be significantly reduced, especially for large-scale boundary value problems, where a large number of degrees of freedom are inevitably involved.

5. Stability Analysis

Based on the sequential scheme described in Section 4, the stability analysis on three levels needs to be inspected, *i.e.* stability of individual solvers, stability of iterations within one step (*i.e.* $k \to k+1$, called *iteration stability* hereafter), stability during time marching (*i.e.* $n \to n+1$, called *staggered stability* hereafter). It should be noted that stability of the former is only a necessary but not sufficient condition for the stability of the latter. Stable individual solvers does not guarantee the stability of iterations between these solvers, nor does a stable pair of solutions at one step guarantee stable solutions during the time marching. A stable iterative scheme requires numerical stability on all the three levels. In this work, the stability analysis of iterations during one step is approached in two ways, one by perturbation theory [9] and the other by error propagation [10]. Detailed analysis is presented as follows.

5.1 Stability of Individual Solvers

As shown in Section 4, the equation of momentum equilibrium is solved explicitly. As proved in [16], with Rayleigh damping used and $\beta \ge \frac{\gamma}{2} \ge \frac{1}{4}$, the mechanics solver is unconditionally stable. The fluid solver with implicit time difference scheme is called once during every iteration, therefore

there is no need to test the stability of flow solver in this level.

5.2 Iteration stability

The iteration stability analysis is approached both by perturbation theory and error propagation method. The formulations with and without stabilization term are both derived to study the effect of stabilization term.

5.2.1 Perturbation theory

Assume a stable pair of solutions ($\mathbf{u}$ and p) is given during each iteration by the two solvers. The fluid equations at two successive iterations $i+1$ and i are given by

$$\left(\mathbf{H}\Delta t_f + \mathbf{S}\right)\mathbf{p}_{n+1}^{(i+1)} + \tilde{\mathbf{S}}\left(\mathbf{p}_{n+1}^{(i+1)} - \mathbf{p}_{n+1}^{(i)}\right) + \mathbf{Q}^T\left(\mathbf{u}_{n+1}^{(i)} - \mathbf{u}_n\right) - \mathbf{S}\mathbf{p}_n - \mathbf{f}_{n+1}^{p}\Delta t_f = 0 \tag{11}$$

$$\left(\mathbf{H}\Delta t_f + \mathbf{S}\right)\mathbf{p}_{n+1}^{(i)} + \tilde{\mathbf{S}}\left(\mathbf{p}_{n+1}^{(i)} - \mathbf{p}_{n+1}^{(i-1)}\right) + \mathbf{Q}^T\left(\mathbf{u}_{n+1}^{(i-1)} - \mathbf{u}_n\right) - \mathbf{S}\mathbf{p}_n - \mathbf{f}_{n+1}^{p}\Delta t_f = 0 \tag{12}$$

Subtracting (12) from (11), it yields

$$\left(\mathbf{H}\Delta t_f + \mathbf{S} + \tilde{\mathbf{S}}\right)\left(\mathbf{p}_{n+1}^{(i+1)} - \mathbf{p}_{n+1}^{(i)}\right) - \tilde{\mathbf{S}}\left(\mathbf{p}_{n+1}^{(i)} - \mathbf{p}_{n+1}^{(i-1)}\right) + \mathbf{Q}^T\left(\mathbf{u}_{n+1}^{(i)} - \mathbf{u}_{n+1}^{(i-1)}\right) = 0 \tag{13}$$

Likewise, the following equation holds for a mechanical system with the essential boundary,

$$-\mathbf{Q}\left(\mathbf{p}_{n+1}^{(i)} - \mathbf{p}_{n+1}^{(i-1)}\right) + \mathbf{K}\left(\mathbf{u}_{n+1}^{(i)} - \mathbf{u}_{n+1}^{(i-1)}\right) = 0 \tag{14}$$

Then the displacement increment during the iteration can be solved as

$$\left(\mathbf{u}_{n+1}^{(i)} - \mathbf{u}_{n+1}^{(i-1)}\right) = \mathbf{K}^{-1}\mathbf{Q}\left(\mathbf{p}_{n+1}^{(i)} - \mathbf{p}_{n+1}^{(i-1)}\right) \tag{15}$$

Inserting (15) into (13), variations of pore fluid pressure during three successive iterations can be expressed as the following,

$$\left(\mathbf{p}_{n+1}^{(i+1)} - \mathbf{p}_{n+1}^{(i)}\right) = \underbrace{\left(\mathbf{H}\Delta t_f + \mathbf{S} + \tilde{\mathbf{S}}\right)^{-1}\left(-\mathbf{Q}^T\mathbf{K}^{-1}\mathbf{Q} + \tilde{\mathbf{S}}\right)}_{\mathbf{A}}\left(\mathbf{p}_{n+1}^{(i)} - \mathbf{p}_{n+1}^{(i-1)}\right) \tag{16}$$

To get a stable and convergent solution of $\mathbf{u}$ and $\mathbf{p}$, the variation of pore fluid pressure during two successive iterations should vanish with iteration continues (while from (15), the variation of displacement also vanishes), which requires that the spectral norm of the amplification matrix $\mathbf{A}$ to be smaller than 1, viz

$$\left\|\mathbf{A}\right\| < 1 \tag{17}$$

With a suitably selected stabilization term $\tilde{\mathbf{S}}$, (17) can be satisfied unconditionally with no limit imposed on the time step size. As is self-evident, the stabilization term would influence the amplification matrix, and therefore influence the convergence rate of the iterations. The closer $\left\|\mathbf{A}\right\|$ approaches zero, the faster the solution converges. Ideally, $\tilde{\mathbf{S}} = \mathbf{Q}^T\mathbf{K}^{-1}\mathbf{Q}$ provides the fastest convergence rate. In this ideal case, the iterative scheme ends after the third iteration, *i.e.*, it obtains

the required solutions in two iterations and needs a third one for tolerance checking.
If the stabilization term is not included, the stability condition requires that the amplification factor must satisfy the following condition

$$\left\| \left(\mathbf{H}\Delta t_f + \mathbf{S} \right)^{-1} \left(-\mathbf{Q}^T \mathbf{K}^{-1} \mathbf{Q} \right) \right\| < 1 \tag{18}$$

For a prescribed boundary value problem, $\mathbf{H}$, $\mathbf{S}$ and $\mathbf{K}$ usually remain unchanged, therefore the range of time step Δt_f for a stable iterative scheme is constrained by (18). The scheme is thus conditionally stable when the stabilization term is not introduced.

5.2.2 *Error propagation method*

Denote by $\left(\tilde{\mathbf{p}}, \tilde{\mathbf{u}} \right)$ the true solutions. $\mathbf{r}_{n+1}^p$ and $\mathbf{r}_{n+1}^u$ are the local truncation errors due to temporal discretization. Eq.(19) is the flow equation with true solution and truncation error implemented.

$$\left(\mathbf{H}\Delta t_f + \mathbf{S} \right) \tilde{\mathbf{p}}_{n+1} + \tilde{\mathbf{S}} \left(\tilde{\mathbf{p}}_{n+1} - \tilde{\mathbf{p}}_{n+1} \right) + \mathbf{Q}^T \left(\tilde{\mathbf{u}}_{n+1} - \tilde{\mathbf{u}}_n \right) - \mathbf{S}\tilde{\mathbf{p}}_n - \mathbf{f}_{n+1}^p \Delta t_f = \mathbf{r}_{n+1}^p \tag{19}$$

Subtracting (11) from (19) and denoting the pressure error as $\mathbf{e}_n^{p,(i)} = \tilde{\mathbf{p}}_n - \mathbf{p}_n^{(i)}$, it becomes

$$\left(\mathbf{H}\Delta t_f + \mathbf{S} + \tilde{\mathbf{S}} \right) \mathbf{e}_{n+1}^{p,(i+1)} - \tilde{\mathbf{S}} \mathbf{e}_{n+1}^{p,(i)} + \mathbf{Q}^T \left(\mathbf{e}_{n+1}^{u,(i)} - \mathbf{e}_n^u \right) - \mathbf{S}\mathbf{e}_n^p = \mathbf{r}_{n+1}^p \tag{20}$$

Similarly, the displacement error $\mathbf{e}_n^{u,(i)} = \tilde{\mathbf{u}}_n - \mathbf{u}_n^{(i)}$ is given by

$$-\mathbf{Q}\mathbf{e}_{n+1}^{p,(i)} + \mathbf{K}\mathbf{e}_{n+1}^{u,(i)} = \mathbf{r}_{n+1}^u \tag{21}$$

$$-\mathbf{Q}\mathbf{e}_n^p + \mathbf{K}\mathbf{e}_n^u = \mathbf{r}_n^u \tag{22}$$

Subtracting (22) from (21), it reads

$$\mathbf{e}_{n+1}^{u,(i)} - \mathbf{e}_n^u = \mathbf{K}^{-1}\mathbf{Q} \left(\mathbf{e}_{n+1}^{p,(i)} - \mathbf{e}_n^p \right) + \mathbf{K}^{-1} \left(\mathbf{r}_{n+1}^u - \mathbf{r}_n^u \right) \tag{23}$$

Substituting (23) into (20), it yields

$$\left(\mathbf{H}\Delta t_f + \mathbf{S} + \tilde{\mathbf{S}} \right) \mathbf{e}_{n+1}^{p,(i+1)} - \tilde{\mathbf{S}} \mathbf{e}_{n+1}^{p,(i)} + \mathbf{Q}^T \mathbf{K}^{-1} \mathbf{Q} \left(\mathbf{e}_{n+1}^{p,(i)} - \mathbf{e}_n^p \right) + \mathbf{Q}^T \mathbf{K}^{-1} \left(\mathbf{r}_{n+1}^u - \mathbf{r}_n^u \right) - \mathbf{S}\mathbf{e}_n^p = \mathbf{r}_{n+1}^p$$

$$\Rightarrow \underbrace{\left(\mathbf{H}\Delta t_f + \mathbf{S} + \tilde{\mathbf{S}} \right)}_{\mathbf{A}'} \mathbf{e}_{n+1}^{p,(i+1)} = \underbrace{\left(\tilde{\mathbf{S}} - \mathbf{Q}^T \mathbf{K}^{-1} \mathbf{Q} \right)}_{\mathbf{B}'} \mathbf{e}_{n+1}^{p,(i)} + \underbrace{\left(\mathbf{S} + \mathbf{Q}^T \mathbf{K}^{-1} \mathbf{Q} \right)}_{\mathbf{C}'} \mathbf{e}_n^p + \underbrace{\mathbf{r}_{n+1}^p - \mathbf{Q}^T \mathbf{K}^{-1} \left(\mathbf{r}_{n+1}^u - \mathbf{r}_n^u \right)}_{\mathbf{r}'_{n+1}}$$

$$\Rightarrow \mathbf{e}_{n+1}^{p,(i+1)} = \left(\mathbf{A}' \right)^{-1} \mathbf{B}' \mathbf{e}_{n+1}^{p,(i)} + \left(\mathbf{A}' \right)^{-1} \mathbf{C}' \mathbf{e}_n^p + \left(\mathbf{A}' \right)^{-1} \mathbf{r}'_{n+1}$$

$$\Rightarrow \mathbf{e}_{n+1}^{p,(i+1)} = \mathbf{G}\mathbf{e}_{n+1}^{p,(i)} + \mathbf{H}' \mathbf{e}_n^p + \left(\mathbf{A}' \right)^{-1} \mathbf{r}'_{n+1}$$

$$\Rightarrow \mathbf{e}_{n+1}^{p,(i+1)} = \mathbf{G}^{i+1} \mathbf{e}_{n+1}^{p,(0)} + \sum_{l=0}^{i} \mathbf{G}^l \mathbf{H}' \mathbf{e}_n^p + \sum_{l=0}^{i} \mathbf{G}^l \left(\mathbf{A}' \right)^{-1} \mathbf{r}'_{n+1}$$

$$\Rightarrow \mathbf{e}_{n+1}^{p,(i+1)} = \mathbf{G}^{i+1} \mathbf{e}_{n+1}^{p,(0)} + \left(\mathbf{I} - \mathbf{G}^{i+1} \right) \left(\mathbf{I} - \mathbf{G} \right)^{-1} \mathbf{H}' \mathbf{e}_n^p + \left(\mathbf{I} - \mathbf{G}^{i+1} \right) \left(\mathbf{I} - \mathbf{G} \right)^{-1} \left(\mathbf{A}' \right)^{-1} \mathbf{r}'_{n+1} \tag{24}$$

Therefore, to ensure the error does not grow during the iterations (with increasing i), the spectral norm of $\mathbf{G}$ should be

$$\|\mathbf{G}\| = \left\|\left(\mathbf{A}'\right)^{-1}\mathbf{B}'\right\| = \left\|\left(\mathbf{H}\Delta t_f + \mathbf{S} + \tilde{\mathbf{S}}\right)^{-1}\left(\tilde{\mathbf{S}} - \mathbf{Q}^T\mathbf{K}^{-1}\mathbf{Q}\right)\right\| < 1 \tag{25}$$

This stability criterion is identical to that of (17).

5.3 Staggered stability

This part is to prove that the error does not grow during the time marching (i.e. from $t_0 \to t_1 \to \cdots \to t_n$). The error in (24) can be further written as

$$\begin{aligned}
&\mathbf{e}_{n+1}^{p,(i+1)} = \mathbf{G}^{i+1}\mathbf{e}_{n+1}^{p,(0)} + \left(\mathbf{I}-\mathbf{G}^{i+1}\right)\left(\mathbf{I}-\mathbf{G}\right)^{-1}\mathbf{H}'\mathbf{e}_n^p + \left(\mathbf{I}-\mathbf{G}^{i+1}\right)\left(\mathbf{I}-\mathbf{G}\right)^{-1}\left(\mathbf{A}'\right)^{-1}\mathbf{r}'_{n+1} \\
&\Rightarrow \mathbf{e}_{n+1}^{p,(i+1)} = \mathbf{L}_{n+1}\mathbf{e}_{n+1}^{p,(0)} + \mathbf{M}_{n+1}\mathbf{e}_n^p + \mathbf{N}_{n+1}\mathbf{r}'_{n+1} \\
&\Rightarrow \mathbf{e}_{n+1}^{p,(i+1)} = \mathbf{L}_{n+1}\mathbf{e}_{n+1}^{p,(0)} + \sum_{l=0}^{n}\mathbf{M}_{n+1}\cdots\mathbf{M}_{n+1-l}\mathbf{L}_{n-l}\mathbf{e}_{n-l}^{p,(0)} \\
&\qquad + \mathbf{M}_{n+1}\cdots\mathbf{M}_0\mathbf{e}_0^p + \sum_{l=0}^{n}\mathbf{M}_{n+1}\cdots\mathbf{M}_{n+1-l}\mathbf{N}_{n-l}\mathbf{r}'_{n-l} + \mathbf{N}_{n+1}\mathbf{r}'_{n+1}
\end{aligned} \tag{26}$$

If a full iteration (*i.e.* large value of i) is adopted, $\mathbf{L} = \mathbf{G}^i \to 0$; or in the special case that $\mathbf{G} = 0$, $\mathbf{L} = 0$, then the first two terms on the right side in the last equation of (26) vanish. Also considering that the truncation error $\mathbf{r}' \propto O(\Delta t^2)$ [11], to ensure the stability of the staggered procedure, it requires that

$$\|\mathbf{M}\| = \left\|\left(\mathbf{I}-\mathbf{G}^{i+1}\right)\left(\mathbf{I}-\mathbf{G}\right)^{-1}\mathbf{H}'\right\| = \left\|\left(\mathbf{H}\Delta t_f + \mathbf{S} + \mathbf{Q}^T\mathbf{K}^{-1}\mathbf{Q}\right)^{-1}\left(\mathbf{S} + \mathbf{Q}^T\mathbf{K}^{-1}\mathbf{Q}\right)\right\| < 1. \tag{27}$$

Therefore, the staggered procedure is unconditionally stable as long as (25) is satisfied.

6. Numerical Simulations

In this section, a 1D consolidation with elastic medium is carried out to verify the iterative coupling scheme described before. The effects of support sizes on the number of iterations are also demonstrated.

6.1 1D Consolidation with stabilization term

As shown in Figure 1, a 10-m thick saturated elastic medium on an impervious base is subjected to a surface surcharge of $20\,kPa$. Impervious boundaries are assigned to two sides and the base of the domain. A free flow boundary, *i.e.* $p = 0\ kPa$, is assigned to the top surface. Young's modulus of the elastic medium is E=10*Mpa*, Poisson's ratio is $\nu = 0.2$, and the permeability is $5\times10^{-8}\,m/s$. The initial pore water pressure p_0 is 20 *kPa* and effective stress is zero. Support size of 1.5 times of the particle interval is used in the simulations. As derived before, the stabilization term $\tilde{\mathbf{S}} = \mathbf{Q}^T\mathbf{K}^{-1}\mathbf{Q}$ should be used to achieve an optimal convergence rate. However, for mathematical simplicity, $\tilde{\mathbf{S}} = \int_\Omega (\mathbf{N}^p)^T \frac{1}{K}\mathbf{N}^p d\Omega$ is used in the simulation presented here to demonstrate the convergence behavior of the iterative scheme. K is the bulk modulus. The error tolerance are set as $TOL_p = TOL_p = 10^{-3}$. The pore water pressure distribution along the mid-column nodes in the simulation is presented and compared with the analytical solution in Figure 2. The simulation and

analytical results are in good agreement, indicating that the soil-water coupled scheme is effective in solving the consolidation and dissipation problems.

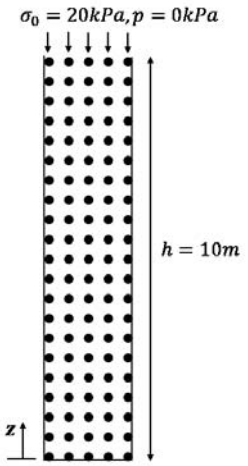

Figure 1. 1D consolidation model setup

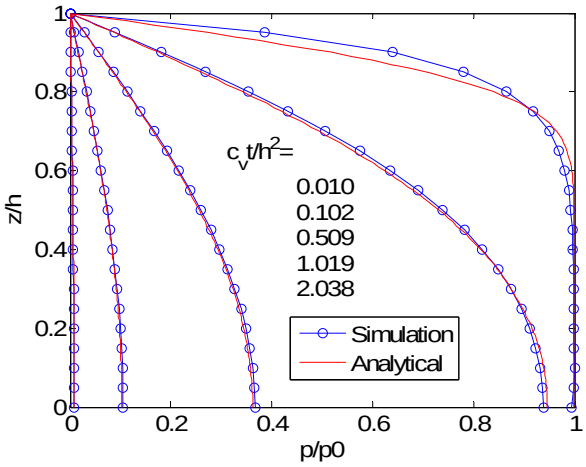

Figure 2. Normalized isochrones distribution of p

Figure 3 present the change of relative error norm during the first 100 iterations. Every line represents the convergence behavior of the relative error norms of **u** and p during one time step. The error norms decrease linearly in a log scale until the prescribed tolerances values are satisfied, i.e., $\left\|\mathbf{p}_{n+1}^{(i+1)}-\mathbf{p}_{n+1}^{(i)}\right\| / \left\|\mathbf{p}_{n+1}^{(i+1)}\right\| \le 10^{-3}$ and $\left\|\mathbf{u}_{n+1}^{(i+1)}-\mathbf{u}_{n+1}^{(i)}\right\| / \left\|\mathbf{u}_{n+1}^{(i+1)}\right\| \le 10^{-3}$. Figure 4 shows the number of iterations needed in each time step of the simulation. In general, convergence can be achieved in around 5 iterations. However, a varying number of iterations are needed in the later part of the simulation.

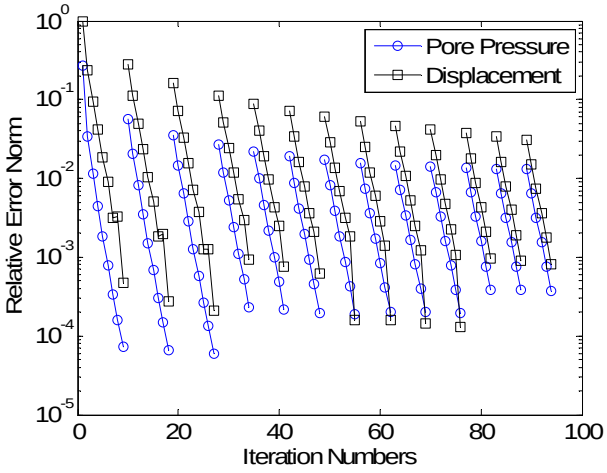

Figure 3 Relative Error Norm

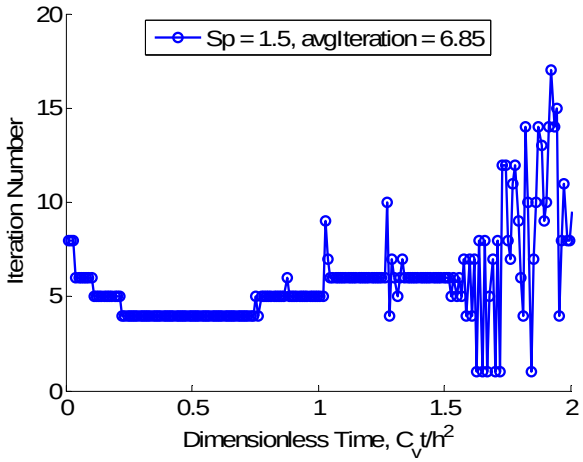

Figure 4. Comparison of iterations numbers

7. Conclusions

A sequential hydro-mechanical coupling scheme using RKPM is presented in this paper. From the stability analysis and numerical simulations, the following conclusions can be drawn

- With a suitably chosen stabilization matrix $\tilde{\mathbf{S}}$, the stabilization technique is proved to be able to effectively make the scheme unconditionally stable. Without the stabilization term, the scheme is proved to be conditionally stable.

- From 1D consolidation simulation case, the solution will effectively converge to the prescribed tolerance during the iterations.
- The effect of stabilization term on the convergence rate should be further explored. An optimal value should be pursued whenever possible.
- The applicability of the iterative scheme for nonlinear problems should be further studied.

Acknowledgements

Funding supports from Research Project Competition (UGC/HKUST) grant No. RPC11EG27 and Direct Allocation Grant DAG08/09.EG01, DGA11EG03G are gratefully acknowledged.

References

[1] C. Felippa, K. Park, Staggered transient analysis procedures for coupled mechanical systems: formulation, Comput. Meth. Appl. Mech. Eng. 24 (1) (1980), 61-111.

[2] O. Zienkiewicz, D. Paul, and A. Chan, Unconditionally stable staggered solution procedure for soil-pore fluid interaction problems, Int. J. Numer. Methods Eng. 26 (5) (1988) 1039-1055 .

[3] B. Schrefler, L. Simoni, and E. Turska, Standard staggered and staggered Newton schemes in thermo-hydro-mechanical problems, Comput. Meth. Appl. Mech. Eng. 144 (1) (1997) 93-109 .

[4] J. Kim, Sequential methods for coupled geomechanics and multiphase flow, Ph.D. thesis, Stanford University (2010).

[5] O. Zienkiewicz, A. Chan, M. Pastor, B.A. Schrefler, T. Shiomi, Computational Geomechanics with Special Reference to Earthquake Engineering: John Wiley (Chichester and New York), 1999.

[6] W. Liu, S. Jun, Y.F. Zhang, Reproducing kernel particle methods, International Journal for Numerical Methods in Fluids 20 (1995) 1081-1106.

[7] S. Li, W. Liu. Meshfree and particle methods and their applications, Applied Mechanics Reviews 55 (2002) 1-34.

[8] T. Hughes, The finite element method: linear static and dynamic finite element analysis, Englewood Cliffs, New Jersey: Prentice-Hall International , Inc., 1987.

[9] T. Belytschko, W. K. Liu, and B. Moran, Nonlinear finite elements for continua and structures. New York: John Wiley & Sons Inc., 2000.

[10] E. Turska, K. Wisniewski, and B. A. Schrefler, Error propagation of staggered solution procedures for transient problems, Computer methods in applied mechanics and engineering 114(1) (1994) 177-188.

[11] E. Turska, and B. A. Schrefler, On convergence conditions of partitioned solution procedures for consolidation problems, Computer methods in applied mechanics and engineering 106(1) (1993) 51-63.